

DiffAlign : Few-shot learning using diffusion based synthesis and alignment

Aniket Roy
Johns Hopkins University
aroy28@jhu.edu

Anshul Shah*
Johns Hopkins University
ashah95@jhu.edu

Ketul Shah*
Johns Hopkins University
kshah33@jhu.edu

Anirban Roy
SRI International
anirban.roy@sri.com

Rama Chellappa
Johns Hopkins University
rchella4@jhu.edu

Abstract

We address the problem of few-shot classification where the goal is to learn a classifier from a limited set of samples. While data-driven learning is shown to be effective in various applications, learning from less data still remains challenging. To address this challenge, existing approaches consider various data augmentation techniques for increasing the number of training samples. Pseudo-labeling is commonly used in a few-shot setup, where approximate labels are estimated for a large set of unlabeled images. We propose DiffAlign which focuses on generating images from class labels. Specifically, we leverage the recent success of the generative models (e.g., DALL-E and diffusion models) that can generate realistic images from texts. However, naive learning on synthetic images is not adequate due to the domain gap between real and synthetic images. Thus, we employ a maximum mean discrepancy (MMD) loss to align the synthetic images to the real images minimizing the domain gap. We evaluate our method on the standard few-shot classification benchmarks: CIFAR-FS, FC-100, miniImageNet, tieredImageNet and a cross-domain few-shot classification benchmark: miniImageNet \rightarrow CUB. The proposed approach significantly outperforms the state-of-the-art in both 5-shot and 1-shot setups on these benchmarks. Our approach is also shown to be effective in the zero-shot classification setup.

1. Introduction

We address the problem of few-shot image classification where the goal is to accurately classify images only using a limited amount of training samples (e.g., 1 to 5 samples) per class. We assume access to a large-scale dataset, usually from the same data distribution but with disjoint class

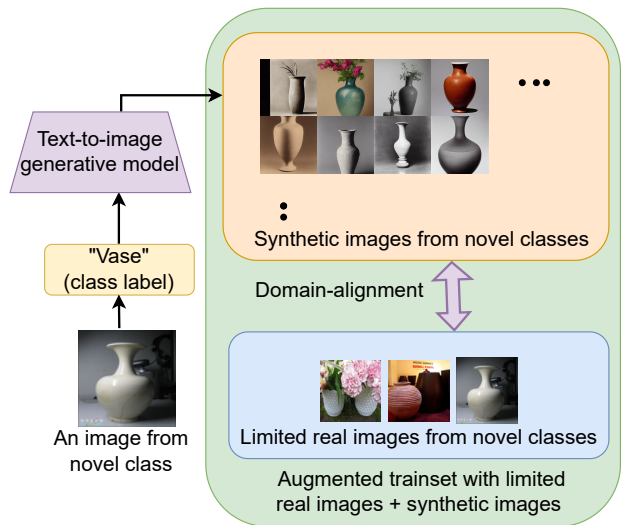


Figure 1. Overview of DiffAlign. We consider a text-to-image generative model, specifically the diffusion model [41], to synthesize a large set of images corresponding to a novel class. The images are generated considering the class labels as text inputs such as ‘vase’ in this example. We align the synthetic images with the real images to reduce the domain gap. Finally, the combined set of limited real images and aligned synthetic images is used to learn a classifier for the novel class.

labels, to allow pre-training of the models. The large-scale set is referred to as the base set and the limited set of novel classes is referred to as the novel set. Thus, the objective of few-shot learning is to develop a transfer technique such that a model, trained on the base set, can adapt to the novel set relying on only a few samples. Few-shot learning is effective in data-scarce scenarios where only limited samples are available and generating additional samples can be expensive such as in medical imaging [50], drug discovery [11], modeling expensive scientific simulations [24].

Supervised image classification approaches have

*Equal contribution

achieved near-human performance [18, 23] leveraging the large-scale datasets [8, 13]. However, learning from limited data remains challenging, especially in few-shot setups, where there are only 1-5 samples available for each class. To address this challenge, existing approaches consider various data augmentation approaches to expand the training set. For example, Jian et al. [21] generate pseudo labels for the base class samples and use these samples for increasing the number of novel class samples. Assoalign [2] uses base-class samples in addition to the novel class samples to generate new samples in an adversarial framework. Roy et al. [43] uses hard-mixup to combine existing samples to generate additional samples.

Inspired by the recent success of the text-to-image generative approaches, such as DALL-E [37] and stable diffusion [41], we propose DiffAlign - an approach to data augmentation where synthetic images are generated using the textual description of the novel classes and aligned with real images for improving few-shot performance. Specifically, we consider the stable diffusion approach [41] that generates realistic images given a text description. We consider class names as text descriptions to generate a large set of synthetic images corresponding to the novel classes. However, directly combining synthetic images with real images may not be effective due to the domain gap between these images. Thus, we propose a maximum mean discrepancy (MMD) loss [28] to align the features of the synthetic images to real images. Along with the aligned synthetic images, we make use of the pseudo-labeling to associate novel-class labels to the base class images [21]. Our experiments indicate that DiffAlign outperforms state-of-the-art approaches on the benchmark datasets in both 5-shot and 1-shot settings. DiffAlign is particularly effective in the 1-shot setting where only one real image is available for each novel class. DiffAlign is also effective in the zero-shot setup where we rely on only the synthetic images.

In the context of few-shot classification, our contributions include:

- We propose a data augmentation strategy by leveraging text-to-image generative models in order to generate synthetic images corresponding to novel classes. This is suitable for the few-shot image classification where only a few images are available for novel classes.
- We propose an MMD-based loss function to align synthetic images to real images in order to reduce the domain gap between real and synthetic images.
- We validate our approach on standard few-shot benchmarks: CIFAR-FS, FC-100, miniImageNet, and tieredImageNet and achieve state-of-the-art performance in both 5-shot and 1-shot setups. In cross-domain few-shot benchmark: miniImageNet \rightarrow CUB,

our approach outperforms the current state-of-the-art. We also demonstrate the efficacy of our approach in the zero-shot setup.

2. Related Work

Few-shot learning methods can be broadly divided into two categories, (1) meta-learning based and (2) transfer learning based.

Meta learning. Meta-learning has been traditionally useful for few-shot learning problems, where the model is trained on the meta-training phase and subsequently tested on the meta-testing phase in a learning-to-learn fashion. To achieve better generalization, usually, multiple episodes are sampled from the task distribution and average performance of the meta-learner is reported. Meta-learning could also be subdivided into two categories, viz., metric-based meta learning and optimization-based meta-learning.

Metric-based meta-learning methods predict the query as the weighted sum of the support samples. Popular metric-based meta-learning methods include Prototypical Networks [47], Relation Networks [49], Matching networks [51], TADAM [33], etc. Another line of optimization-based meta-learning methods adapt the model parameters using a small number of gradient steps, MAML [15], LEO [44], etc. By solving a differentiable convex optimization problem for few-shot learning, MetaOptNet [38] achieves better generalization. Several other meta-learning approaches use earth-mover’s distance [59], set-to-set functions [56], human interpretable concepts [8], etc.

Transfer learning. Instead of traditional meta-learning approaches, recent methods rely on simple yet efficient transfer-learning approach. RFS [50] shows contrastive pre-training on the large base dataset and simple finetuning on the novel examples outperforms all the meta-learning baselines. SKD [36] added rotational self-supervised distillation to further improve the performance. Using complementary strengths of invariant and equivariant representations and self-distillation, Rizve et al. [40] performs significantly better than previous few-shot learning methods. Feature-level knowledge distillation using partner-assisted learning [29] has proven to be effective. Recent few-shot classification techniques use - co-adaptation of discriminative features [10], mutual centralized learning [27], discriminative subspace [63], multi-task representation learning [6], contrastive learning [55], task-aware dynamic kernels [30], CLIP adaptation [61] and large pretrained networks [20].

Data augmentation for few-shot learning. Recent methods use readily available base dataset in addition to novel class samples. AssoAlign [2] selects nearest neighbors of the novel class samples from the abundant base dataset and adversarially align those for training. Jian et

al. [21] pseudolabel the entire base dataset using a classifier trained on the novel classes. Roy et al. [43] use hard-mixup sample selection to further improve the performance. Afrasiyabi et al. [3] approaches few-shot classification using mixture-based feature space learning [3] and matching feature sets [4]. However, these approaches have not used the text label information.

Multi-modal few-shot learning. Semantic information seems to improve few-shot classification [1]. Padhe et al. [34] use multi-modal prototypical networks for few-shot classification. Consecutively, Yang et al. [54] utilize semantic guided attention to integrate the rich semantics into few-shot classification. Xu et al. [53] generates representative samples for few-shot learning using text-guided variational autoencoder. Wang et al. [52] uses multi-directional knowledge transfer for multi-modal few-shot learning. Text-guided prototype completion [58] also helps few-shot classification.

Vision-language models. Recent advancements in large-scale vision language pretrained models enable significant improvements in multi-modal learning with CLIP [35], GPT-3 [7], DALLE [37], stable diffusion [41] etc. Diffusion models are state-of-the-art text-to-image generative models [19, 32, 37, 41], which are trained on large-scale image and text corpus and produces surprisingly well images just from texts.

We consider a combination of data augmentation and alignment approach to generate a large number of realistic images and align them closely with the real images. Training the classifier on the combined set ensures high prediction accuracy for the novel classes.

3. Problem Formulation

Following the standard practice, we formulate the few-shot classification problem as follows. We assume access to a large-scale labeled base dataset and the goal is to classify novel classes using a limited set of training images from the novel set. The task is to learn feature representations using the base dataset with abundant samples and then adapt to classify novel classes using only a few samples.

We denote the base dataset as $\mathcal{D}^{\text{base}} = \{x_t^{\text{base}}, y_t^{\text{base}}\}_{t=1}^{N^{\text{base}}}$, where x_t^{base} is an image from base classes and the corresponding label is $y_t^{\text{base}} \in C^{\text{base}}$. Similarly, we denote the novel dataset as $\mathcal{D}^{\text{novel}} = \{x_t^{\text{novel}}, y_t^{\text{novel}}\}_{t=1}^{N^{\text{novel}}}$, where x_t^{novel} is an image of novel classes and the corresponding label is $y_t^{\text{novel}} \in C^{\text{novel}}$. The base classes and novel classes are disjoint, i.e., $C^{\text{base}} \cap C^{\text{novel}} = \emptyset$, and usually $|C^{\text{base}}| \geq |C^{\text{novel}}|$.

The training and testing are performed in episodes on the novel class images. Each episode i addresses an N -way K -shot problem where the few-shot classifier is trained on a support set, i.e., $\mathcal{D}_i^{\text{support}} = \{x_{i,t}^{\text{support}}, y_{i,t}^{\text{support}}\}_{t=1}^{NK}$

to classify N novel classes containing K images per class. Then, the few-shot classifier is evaluated on a query set $\mathcal{D}_i^{\text{query}} = \{x_{i,t}^{\text{query}}, y_{i,t}^{\text{query}}\}_{t=1}^{NK}$ to classify the same N classes. K is usually set to 1 and 5 for 1-shot and 5-shot setups, respectively and N is usually set to 5.

4. Proposed Approach

We propose DiffAlign which uses the diffusion method [41] for data augmentation where synthetic images are generated using the textual description of the novel classes and aligned with real images such that the synthetic images can be effectively used in training a few-shot classifier. Our approach has five main components: 1) learning a classifier on the base dataset, 2) generating pseudo labels for the base dataset, 3) data augmentation by generating synthetic images for novel classes, 4) aligning synthetic images with real images, and 5) training a few-shot classifier on the combined dataset. We describe these components below.

4.1. Learning a classifier on the base dataset

We start with learning a discriminative classifier on the base dataset $\mathcal{D}^{\text{base}}$. Following the self-supervised invariant and equivariant representation learning (IER) framework [40], we perform a contrastive pretraining on the base dataset using a self-supervised loss. This is followed by a class-wise training with a cross-entropy classification loss (L_{CE}). We consider a ResNet model [18] as $f_{\theta}(\cdot)$, parameterized by θ . The network is learned using the cross-entropy loss on the base dataset $\mathcal{D}^{\text{base}}$.

$$\theta^{\text{base}} = \operatorname{argmin}_{\theta} \mathbb{E}_{\{x,y\} \in \mathcal{D}^{\text{base}}} L_{CE}(f_{\theta}(x), y) \quad (1)$$

4.2. Generating pseudo labels for the base dataset

Next, we leverage the large-scale base dataset that shares the same distribution as the novel dataset. We employ the pseudo-labeling approach which is shown to be effective for few-shot setups [21]. Specifically, we train a logistic regression classifier (g_{ϕ}) using the limited images from novel classes. Then, the trained classifier is used to predict the labels of the images from the base dataset. The predicted labels are considered pseudo labels. The base images with pseudo labels are considered as additional images along with the few novel class images to train the classifier (h_{ϕ}). In each episode i , we learn a classifier $g_{\phi_i}(\cdot)$ using the support set of novel examples $\mathcal{D}_i^{\text{support}}$ with the cross-entropy loss, such that

$$\phi_i = \operatorname{argmin}_{\phi} \mathbb{E}_{\{x,y\} \in \mathcal{D}_i^{\text{support}}} L_{CE}(g_{\phi}(f_{\theta^{\text{base}}}(x)), y). \quad (2)$$

Note that the classifier for the novel classes is learned based on the features extracted using the base class classifier $f_{\theta^{\text{base}}}(\cdot)$ in Eq. 1. The classifier g_{ϕ_i} is used to generate pseudo-labels for the entire base dataset, i.e., $\hat{y}_t^{\text{base}} = g_{\phi_i}(f_{\theta^{\text{base}}}(x_t))$ for $t = 1, \dots, N^{\text{base}}$.

We randomly sample a set of the base set images and the corresponding softmax distribution over the pseudo-labels to compute the KL divergence loss \mathcal{L}_{base} that is to be minimized

$$\mathcal{L}_{base} = KL(h_\phi(f_\theta(x^{base})), \hat{y}^{base}) \quad (3)$$

4.3. Data augmentation by generating synthetic images for novel classes

Data augmentation is an important part of a few-shot classification framework as this helps expand the training samples for the novel classes. Recently, text-guided data augmentation techniques are shown to be effective in multi-modal few-shot learning [34, 53, 55]. Current text-to-image generative models have shown impressive performance in generating realistic images from text descriptions. We employ these models to generate a large number of synthetic images corresponding to the novel classes. We consider the diffusion models [41] to generate synthetic images considering novel class names as the text description. Considering class name as the prompt for the generative models is shown to be effective [62]. To the best of our knowledge, we are first to investigate the effectiveness of the generated synthetic images for few-shot and zero-shot classification tasks. We briefly describe the image generation process using diffusion models.

Diffusion models. Diffusion models [19, 32, 37, 41] are state-of-the-art generative models that are trained on large-scale datasets and generate realistic images from free-form texts. Compared to other generative models, e.g. GANs [17], flow-based models [22], diffusion models are more stable and produce more realistic images. In this work, we consider the stable diffusion [41]. We start with an input image x and gradually add Gaussian noise to generate a noisy image x_t . Then a denoising autoencoder is trained to recover the original data by reversing the noising process. Since the goal is to learn the data distribution $p(x)$, the denoising autoencoder is trained to minimize the variational lower bound of $p(x)$. Due to the Gaussian noise assumption, these models can be represented as an equally weighted sequence of denoising autoencoder ($\epsilon_\theta(x_t, t)$) corresponding to each denoising step $t = 1, \dots, T$. Therefore, the corresponding objective function can be expressed as,

$$L_{DM} = \mathbb{E}_{x, \epsilon \sim \mathcal{N}(0,1), t} [\|\epsilon - \epsilon_\theta(x_t, t)\|_2^2] \quad (4)$$

Instead of applying the diffusion process on the high-dimensional input, Rombach et al. [41] propose to project inputs to a lower latent dimension representation and apply diffusion on this. Let's denote the latent space is $z_t = G(x_t)$, where $G(\cdot)$ is the UNet-style encoder [42]. Then the latent diffusion loss is given as

$$L_{LDM} = \mathbb{E}_{G(x), \epsilon \sim \mathcal{N}(0,1), t} [\|\epsilon - \epsilon_\theta(z_t, t)\|_2^2] \quad (5)$$

For text-conditioned image generation, a domain-specific encoder is used (τ_θ) which projects class names (y) to an intermediate representation that is mapped to the intermediate layers of the UNet [42] via a cross-attention layer. Finally, the text-conditional diffusion model is trained jointly using the loss [41] as

$$L_{LDM} = \mathbb{E}_{G(x), y, \epsilon \sim \mathcal{N}(0,1), t} [\|\epsilon - \epsilon_\theta(z_t, t, \tau_\theta(y))\|_2^2] \quad (6)$$

Stable diffusion. Stable diffusion is a diffusion model conditioned on text embedding of CLIP ViT-L/14 [35] text encoder and trained on LAION-400M dataset [41] using image-text pairs. The stable diffusion model can generate realistic images from text descriptions. Therefore, we pass the novel class names (y^{novel}) as text prompts to the stable diffusion to generate semantically meaningful synthetic images (x^{syn}). Some examples of the realistic generated synthetic images are shown in Fig. 5.

Now, we use these generated samples to train the few-shot classifier. Note, we use label smoothing in the cross-entropy loss ($L_{CE_{smooth}}$) to regularize the model to avoid overfitting. Thus the loss corresponding to synthetic images becomes:

$$\mathcal{L}_{syn} = L_{CE_{smooth}}(h_\phi(f_\theta(x^{syn})), y^{novel}) \quad (7)$$

4.4. Aligning synthetic images with real images

Despite the high-quality synthetic images, there exist a domain gap between the real and synthetic images in terms of the background, color and intensity distribution as shown in Fig. 6c. The average color histograms of the real and synthetic images are shown in Fig. 3, which exhibits a distinction between these set of images. To mitigate this, we use a multi-kernel Maximum Mean Discrepancy (MMD) loss to reduce the domain gap.

Let's assume, given a source (\mathcal{D}_s) and target domain (\mathcal{D}_t), samples are drawn from these domains with the distribution P and Q , respectively over a set \mathcal{X} . The features of the samples from these domains are denoted as $\{z_i^s\}$ and $\{z_i^t\}$, respectively. A multi-kernel MMD ($D_k(P, Q)$) between probability distributions P and Q is defined as [28],

$$D_k(P, Q) = \|\mathbb{E}_p[\psi(z^s)] - \mathbb{E}_q[\psi(z^t)]\|_{\mathcal{H}_k}^2 \quad (8)$$

where k is the kernel function in the functional space,

$$k = \sum_{p=1}^P \alpha_p k_p \quad (9)$$

where k_p is a single kernel. The feature map $\psi : \mathcal{X} \rightarrow \mathcal{H}_k$ maps into a reproducing kernel Hilbert space. We use three Gaussian kernels with standard deviation, $\alpha = 0.5, 1, 2$, thus $k = \{\mathcal{N}(0, 0.5), \mathcal{N}(0, 1), \mathcal{N}(0, 2)\}$. If the kernel is $k(x, y) = \langle \psi(x), \psi(y) \rangle_{\mathcal{H}_k}$, then using kernel trick,

MMD can be estimated as without directly learning $\psi(\cdot)$ as

$$\bar{D}_k(P, Q) = \frac{1}{n_s^2} \sum_{i=1}^{n_s} \sum_{j=1}^{n_s} k(z_i^s, z_j^s) + \frac{1}{n_t^2} \sum_{i=1}^{n_t} \sum_{j=1}^{n_t} k(z_i^t, z_j^t) - \frac{2}{n_s n_t} \sum_{i=1}^{n_s} \sum_{j=1}^{n_t} k(z_i^s, z_j^t) \quad (10)$$

Therefore, the MMD-loss between the real novel examples (x^{novel}) and synthetic examples (x^{syn}) will be,

$$\mathcal{L}_{MMD} = \bar{D}_k(f_\theta(x^{novel}), f_\theta(x^{syn})) \quad (11)$$

4.5. Training the few-shot classifier

Finally, we train the entire backbone (f_θ) and the classifier (g_ϕ) using 1) cross-entropy loss on the novel samples: $\mathcal{L}_{novel} = L_{CE}(h_\phi(f_\theta(x^{novel})), y^{novel})$, 2) cross-entropy loss with label smoothing on the generated synthetic images: \mathcal{L}_{syn} (Eq. 7), 3) KL-divergence loss on the base samples with their corresponding pseudo-labels: \mathcal{L}_{base} (Eq. 3), and 4) MMD loss with novel samples and generated synthetic samples: \mathcal{L}_{MMD} (Eq. 11).

Hence, the the loss function is given as

$$\mathcal{L} = \alpha_1 \cdot \mathcal{L}_{novel} + \alpha_2 \cdot \mathcal{L}_{syn} + \alpha_3 \cdot \mathcal{L}_{base} + \alpha_4 \cdot \mathcal{L}_{MMD} \quad (12)$$

We set $\alpha_1 = 1$, $\alpha_2 = 1$, $\alpha_3 = 1$ and $\alpha_4 = 0.05$ in our experiments.

4.6. Implementation details

For a fair comparison, we use ResNet-12 architecture as the backbone network. On top of the feature extractor, we add a two-layer MLP to perform N-way classification. A stochastic gradient descent optimizer is used with a momentum of 0.9, and the learning rate of the backbone and the classifier has been set as 0.025 and 0.05 respectively with weight decay of 5e-4. Standard data augmentations e.g., color jittering, random crop, and horizontal flip are employed during training in a minibatch of 250 images. More details are provided in the supplementary material.

5. Experiments

Datasets and metric. We experiment on the four common few-shot benchmarks : FC-100 [33], CIFAR-FS [5], miniImageNet [51] and tieredImageNet [39]. FC-100 is a subset of CIFAR-100, containing 60 classes for meta-training, 20 classes for meta-validation and 20 classes for meta-testing. CIFAR-FS is also obtained from CIFAR-100, containing 64 classes for meta-training, 16 classes for meta-validation and 20 classes for meta-testing. miniImageNet is derived from ImageNet with images downsampled to a resolution of 84×84 pixels. It has 64 classes for meta-training,

16 classes for meta-validation and 20 classes for meta-testing. tieredImageNet [39] is another subset of ImageNet, containing total of 608 classes, from which 351 classes are used for meta-training, 97 classes for meta-validation and 160 classes for meta-testing. Following standard practice, we consider the classification accuracy as the metric.

Table 1. Comparison of DiffAlign (ours) to prior works on CIFAR-FS. Following prior work, we report our results with 95% confidence intervals on meta-testing split of the dataset. § denotes our reproduced numbers using publicly available implementations.

Model	Backbone	CIFAR-FS 5-way	
		1-shot	5-shot
ProtoNet [47] (NIPS'17)	ResNet-12	72.2 ± 0.7	83.5 ± 0.5
MetaOptNet [25] (CVPR'19)	ResNet-12	72.6 ± 0.7	84.3 ± 0.5
Shot-Free [38] (ICCV'19)	ResNet-12	69.2 ± n/a	84.7 ± n/a
DSN-MR [46] (CVPR'20)	ResNet-12	75.6 ± 0.9	86.2 ± 0.6
RFS-simple [50] (ECCV'20)	ResNet-12	71.5 ± 0.8	86.0 ± 0.5
RFS-distill [50] (ECCV'20)	ResNet-12	73.9 ± 0.8	86.9 ± 0.5
SKD-GEN1 [36] (Arxiv'20)	ResNet-12	76.6 ± 0.9	88.6 ± 0.5
IER-distill [40] (CVPR'21)	ResNet-12	77.6 ± 1.0	89.7 ± 0.6
PAL [29] (ICCV'21)	ResNet-12	77.1 ± 0.7	88.0 ± 0.5
Label-Halluc [21] (AAAI'22)	ResNet-12	78.0 ± 1.0 [§]	89.37 ± 0.6 [§]
FeLMi [43] (NeurIPS'22)	ResNet-12	78.22 ± 0.7	89.47 ± 0.5
SEGA [54] (WACV'22)	ResNet-12	78.45 ± 0.24	86.00 ± 0.2
SVAE [53] (CVPR'22)	ResNet-12	73.25 ± 0.44	78.89 ± 0.34
DiffAlign (Ours)	ResNet-12	88.99 ± 0.8 (+10.54%)	91.96 ± 0.5 (+2.26%)

Table 2. Comparison of DiffAlign to prior works on FC-100. Following prior work, we report our results with 95% confidence intervals on meta-testing split of the dataset. § denotes our reproduced numbers using publicly available implementations.

Model	Backbone	FC-100 5-way	
		1-shot	5-shot
ProtoNet [47] (NIPS'17)	ResNet-12	37.5 ± 0.6	52.5 ± 0.6
TADAM [33] (NIPS'18)	ResNet-12	40.1 ± 0.4	56.1 ± 0.4
MetaOptNet [25] (CVPR'19)	ResNet-12	41.1 ± 0.6	55.5 ± 0.6
MTL [48] (CVPR'19)	ResNet-12	45.1 ± 1.8	57.6 ± 0.9
DeepEMD [59] (CVPR'20)	ResNet-12	46.5 ± 0.8	63.2 ± 0.7
RFS-simple [50] (ECCV'20)	ResNet-12	42.6 ± 0.7	59.1 ± 0.6
RFS-distill [50] (ECCV'20)	ResNet-12	44.6 ± 0.7	60.9 ± 0.6
AssoAlign [2] (ECCV'20)	ResNet-18	45.8 ± 0.5	59.7 ± 0.6
SKD-GEN1 [36] (Arxiv'20)	ResNet-12	46.5 ± 0.8	64.2 ± 0.8
InfoPatch [16] (AAAI'21)	ResNet-12	43.8 ± 0.4	58.0 ± 0.4
IER-distill [40] (CVPR'21)	ResNet-12	48.1 ± 0.8	65.0 ± 0.7
PAL [29] (ICCV'21)	ResNet-12	47.2 ± 0.6	64.0 ± 0.6
Label-Halluc [21] (AAAI'22)	ResNet-12	47.37 ± 0.7 [§]	67.92 ± 0.7 [§]
FeLMi [43] (NeurIPS'22)	ResNet-12	49.02 ± 0.7	68.68 ± 0.7
SVAE [53] (CVPR'22)	ResNet-12	45.75 ± 0.4	54.44 ± 0.4
DiffAlign (Ours)	ResNet-12	69.37 ± 0.7 (+20.35%)	76.12 ± 0.7 (+7.44%)

Comparison with the state-of-the-art.

Few-shot setup. Comparisons on CIFAR-FS, FC-100, miniImageNet, and tieredImageNet in both 5-way 1-shot and 5-way 5-shot settings are provided in Table. 1, Table. 2, Table. 3, respectively. DiffAlign consistently outperforms the state-of-the-art on these datasets. We particularly achieve better performance in a 5-way 1-shot setting where the implication of the augmented images is more prominent.

Zero-shot setup. Since our approach uses class names to generate synthetic images, it is also applicable to zero-shot setup. In Table. 5, we show the zero-shot performance. Our approach is comparable to the competitive baselines,

Table 3. Comparison of our method (DiffAlign) against the state-of-the-art on miniImageNet and tieredImageNet. Following prior work, we report our results with 95% confidence intervals on meta-testing split of the dataset. § denotes our reproduced numbers using publicly available implementations.

Model	Backbone	miniImageNet 5-way		tieredImageNet 5-way	
		1-shot	5-shot	1-shot	5-shot
ProtoNet [47] (NIPS'17)	ResNet-12	60.37 ± 0.83	78.02 ± 0.57	65.65 ± 0.92	83.40 ± 0.65
TADAM [33] (NIPS'18)	ResNet-12	58.50 ± 0.30	76.70 ± 0.30	-	-
TapNet [57] (ICML'19)	ResNet-12	61.65 ± 0.15	76.36 ± 0.10	63.08 ± 0.15	80.26 ± 0.12
MetaOptNet [25] (CVPR'19)	ResNet-12	62.64 ± 0.61	78.63 ± 0.46	65.99 ± 0.72	81.56 ± 0.53
MTL [48] (CVPR'19)	ResNet-12	61.20 ± 1.80	75.50 ± 0.80	65.62 ± 1.80	80.61 ± 0.90
Shot-Free [38] (ICCV'19)	ResNet-12	59.04 ± 0.43	77.64 ± 0.39	66.87 ± 0.43	82.64 ± 0.43
DSN-MR [46] (CVPR'20)	ResNet-12	64.60 ± 0.72	79.51 ± 0.50	67.39 ± 0.83	82.85 ± 0.56
DeepEMD [59] (CVPR'20)	ResNet-12	65.91 ± 0.82	82.41 ± 0.56	71.16 ± 0.87	86.03 ± 0.58
FEAT [56] (CVPR'20)	ResNet-12	66.78 ± 0.20	82.05 ± 0.14	70.80 ± 0.23	84.79 ± 0.16
Neg-Cosine [26] (ECCV'20)	ResNet-12	63.85 ± 0.81	81.57 ± 0.56	-	-
RFS-simple [50] (ECCV'20)	ResNet-12	62.02 ± 0.63	79.64 ± 0.44	69.74 ± 0.72	84.41 ± 0.55
RFS-distill [50] (ECCV'20)	ResNet-12	64.82 ± 0.82	82.41 ± 0.43	71.52 ± 0.69	86.03 ± 0.49
AssoAlign [2] (ECCV'20)	ResNet-18	59.88 ± 0.67	80.35 ± 0.73	69.29 ± 0.56	85.97 ± 0.49
AssoAlign [2] (ECCV'20)	WRN-28-10	65.92 ± 0.60	82.85 ± 0.55	-	-
SKD-GEN1 [36] (Arxiv'20)	ResNet-12	66.54 ± 0.97	83.18 ± 0.54	72.35 ± 1.23	85.97 ± 0.63
P-Transfer [45] (AAAI'21)	ResNet-12	64.21 ± 0.77	80.38 ± 0.59	-	-
MELR [14] (ICLR'21)	ResNet-12	67.40 ± 0.43	83.40 ± 0.28	72.14 ± 0.51	87.01 ± 0.35
IEPT [60] (ICLR'21)	ResNet-12	67.05 ± 0.44	82.90 ± 0.30	72.24 ± 0.50	86.73 ± 0.34
IER-distill [40] (CVPR'21)	ResNet-12	66.85 ± 0.76	84.50 ± 0.53	72.71 ± 0.89	86.57 ± 0.81
Label-Halluc [21](AAAI'22)	ResNet-12	67.04 ± 0.7 [§]	85.87 ± 0.48 [§]	71.97 ± 0.89	86.80 ± 0.58
FeLMi [43] (NeurIPS'22)	ResNet-12	67.47 ± 0.78	<u>86.08 ± 0.44</u>	71.63 ± 0.89	<u>87.07 ± 0.55</u>
SEGA [54] (WACV'22)	ResNet-12	69.04 ± 0.26	79.03 ± 0.18	72.18 ± 0.3	84.28 ± 0.21
SVAE [53] (CVPR'22)	ResNet-12	<u>72.79 ± 0.19</u>	80.70 ± 0.16	<u>73.90 ± 0.24</u>	84.17 ± 0.18
DiffAlign (Ours)	ResNet-12	82.81 ± 0.8 (+10.02%)	88.63 ± 0.3 (+2.55%)	76.87 ± 0.8 (+2.97%)	88.09 ± 0.6 (+1.02%)

Table 4. Comparison of DiffAlign (ours) in cross-domain setting (miniImageNet → CUB). We obtain significant boost compared to prior approaches showing the efficacy of our approach.

Model	Backbone	miniImageNet → CUB 5-way	
		1-shot	5-shot
Baseline++ [9] (ICLR'19)	ResNet-18	40.44 ± 0.75	56.64 ± 0.72
MetaOptNet [25] (CVPR'19)	ResNet-18	44.79 ± 0.75	64.98 ± 0.68
S2M2R [31] (WACV'20)	ResNet-18	48.24 ± 0.84	70.44 ± 0.75
AssoAlign [2] (ECCV'20)	ResNet-18	47.25 ± 0.76	72.37 ± 0.89
MixFSL [3] (ICCV'21)	ResNet-18	-	68.77 ± 0.9
MT-ConFT [12] (ICCV'21)	ResNet-10	49.25 ± 0.83	74.45 ± 0.71
FeLMi [43] (NeurIPS'22)	ResNet-12	51.66 ± 0.82	77.61 ± 0.69
DiffAlign (Ours)	ResNet-12	75.1 ± 0.82 (+23.44%)	85.18 ± 0.68 (+7.57%)

Table 5. Comparison of zero-shot performance with few shot approaches.

Dataset	5-way 1-shot			5-way 0-shot
	IER-distill [40]	Label-Halluc [21]	DiffAlign	DiffAlign
CIFAR-FS	77.6 ± 1.0	78.0 ± 1.0	88.99 ± 0.8	82.01 ± 0.5
FC-100	48.1 ± 0.8	47.37 ± 0.7	69.37 ± 0.7	64.06 ± 0.7
miniImageNet	66.85 ± 0.7	67.04 ± 0.7	82.81 ± 0.8	75.94 ± 0.5
tieredImageNet	72.71 ± 0.8	71.97 ± 0.8	76.87 ± 0.8	62.86 ± 0.6

e.g., IER [40], LabelHalluc [21] for 5-way 1-shot that considers one image per class. This justifies the efficacy of our approach in zero-shot setup.

Cross-domain benchmarks. We evaluate on cross-domain few-shot benchmark miniImageNet → CUB. In this setting, the base-pretraining is done on miniImageNet

Table 6. Performance comparison of adding synthetic vs real images on miniImageNet

Setting	Accuracy
5-way 5-shot	84.50 ± 0.53
5-way 5-shot + 5 synthetic aug	87.36 ± 0.40
5-way 10-shot	89.32 ± 0.40

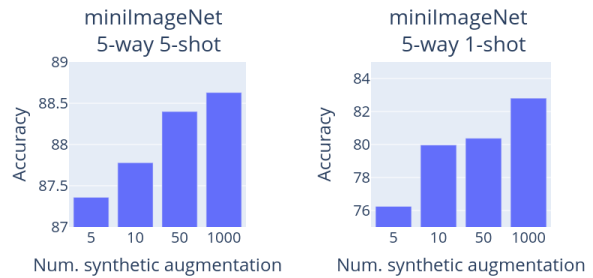


Figure 2. Variation of performance w.r.t the generated augmented samples for miniImageNet

and the novel classes are from the fine-grained CUB dataset. We outperform the state-of-the-art approaches in both 5-way 5-shot and 5-way 1-shot setups as shown in Table 4. We present examples of generated fine-grained bird species in Fig. 5 which shows the effectiveness of the data gener-

Table 7. Ablation on losses

Losses	FC-100		CIFAR-FS		miniImageNet	
	5w1s	5w5s	5w1s	5w5s	5w1s	5w5s
\mathcal{L}_{novel}	48.1 ± 0.8	65.0 ± 0.7	77.6 ± 1.0	89.71 ± 0.6	66.85 ± 0.76	84.50 ± 0.53
$\mathcal{L}_{novel} + \mathcal{L}_{syn}$	67.33 ± 0.7	73.11 ± 0.7	86.33 ± 0.8	90.87 ± 0.5	80.92 ± 0.7	85.05 ± 0.48
$\mathcal{L}_{novel} + \mathcal{L}_{syn} + \mathcal{L}_{base}$	69.18 ± 0.7	75.99 ± 0.7	88.9 ± 0.8	91.83 ± 0.5	82.16 ± 0.7	87.88 ± 0.5
$\mathcal{L}_{novel} + \mathcal{L}_{syn} + \mathcal{L}_{base} + \mathcal{L}_{MMD}$	69.37 ± 0.7	76.12 ± 0.7	88.99 ± 0.8	91.96 ± 0.5	82.81 ± 0.8	88.63 ± 0.3

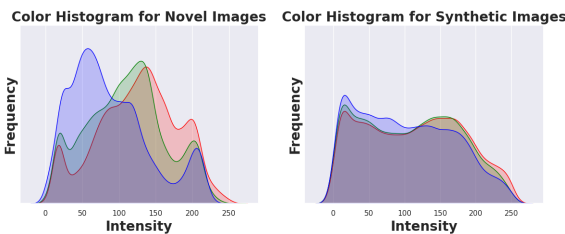


Figure 3. Color histogram of novel and synthetic samples

ative approach for a challenging fine-grained setup where classes can be similar.

Comparison with real vs synthetic images. We compare the effectiveness of the generated samples vs real data. For evaluation, we consider two experiment setups: 5-way 5-shot + 5 augmentation per class with 5 real and 5 synthetic images and 5-way 10-shot with 10 real images. The comparison on miniImageNet is shown in Table. 6. Note that with the domain alignment, few-shot performance with 5-way 5-shot + 5 augmentation is comparable to 5-way 10-shot.

Ablation study on the losses. We conduct an ablation study on the loss functions in Table. 7. As expected, data augmentation in terms of generating synthetic images and pseudo-labeling base samples are shown to be important for few-shot setups. Domain alignment through the MMD loss is also useful to further improve performance. The effect of the MMD loss is also evident in Fig. 4 where the distance between synthetic and real images is reduced as training progresses.

Effect on the synthetic samples. We explore the dependency of the performance on the number of per-class synthetic images. We evaluate on miniImageNet for both 5-shot and 1-shot setups. As expected, the performance gradually improves with the number of generated samples as shown in Fig. 2.

Failure analysis and limitations. Even though the diffusion models are able to generate realistic and diverse images, the domain gap between the real and synthetic images can pose challenges for few-shot classifiers. This can only partially be mitigated by the MMD loss. For example, we randomly consider an episode of a 5-way 5-shot learning and observe class-wise performance and the gen-

erated synthetic images. As shown in Fig. 6a, the accuracy of the ‘lion’ class is particularly low, and generated images, that are gray-scale focused on the face, are quite different from the real images. The accuracy is improved slightly with MMD loss. However, making further improvements require better synthetic samples. We present the average color histogram for real and synthetic images in Fig. 3 that further illustrates the domain gap.

Beyond the difference in appearance, in some cases, generated images are semantically different from the target classes. We present a few of such images in the 4th and 5th row of Fig. 7. For example, in the case of the ‘hey’ and ‘electric ray’ classes, images of trucks and electric instruments are generated. The proposed MMD loss is perhaps not sufficient to reduce this type of semantic gap. One can consider a detailed text description of the classes instead of just the class name to generate diverse semantically related images.

6. Conclusion

We have proposed DiffAlign - a data-augmentation approach for few-shot classification exploiting the recent text-to-image generative models. As there are only a few images available in a few-shot setup, we generate realistic images using the class name as the text description. Our study has shown that the domain gap between the real and synthetic images can pose challenges to a few-shot learner. To mitigate this, we have proposed a multi-kernel MMD based loss function to align synthetic images to the real images. DiffAlign has outperformed state-of-the-art approaches on standard few-shot classification benchmarks, such as FC-100, CIFAR-FS, miniImageNet, tieredImageNet, in both 5-shot and 1-shot setups. DiffAlign is particularly effective in 1-shot or zero-shot setups, where data augmentation is more useful. We have performed ablation studies to justify the contribution of various components of our approach. Finally, we investigate the failure cases and discuss the limitations of our approach.

References

- [1] Mohamed Afham, Salman Khan, Muhammad Haris Khan, Muzammal Naseer, and Fahad Shahbaz Khan. Rich

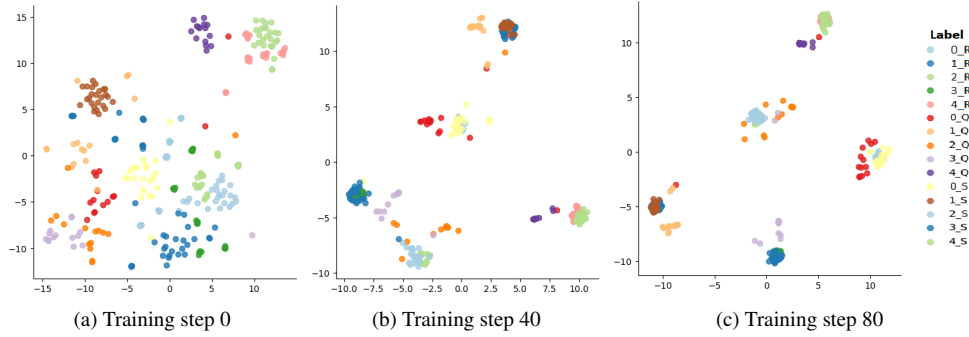


Figure 4. tSNE plot for the image representations across the training iterations. For a 5-way problem, class labels are marked from 0 to 4. For class c , corresponding real support images, synthetically generated images, and query images are denoted by c_R , c_S and c_Q , respectively. We notice that as the training progresses, the representations of the real novel images and synthetic novel images are getting closer, thus reducing the domain gap. Moreover, both the novel samples and the synthetic samples are concentrated toward the query samples, which depicts the discriminative power of the few-shot classifier.

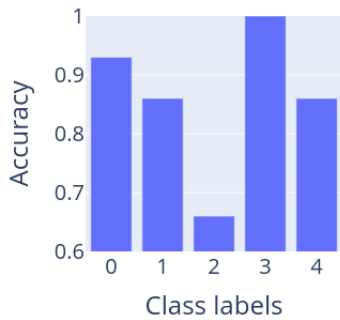


Figure 5. Real and generated images from CUB dataset. Note the synthetic images are generated from class labels only. The categories are: American pipit (first row), Black throated Blue Warbler (second row), Brown Pelican (third row).

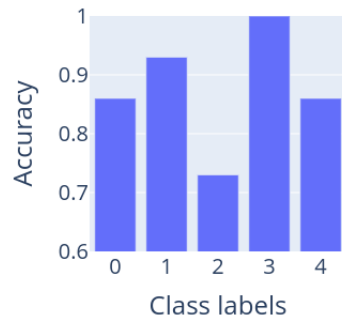
semantics improve few-shot learning. *arXiv preprint arXiv:2104.12709*, 2021. 3

- [2] Arman Afrasiyabi, Jean-François Lalonde, and Christian Gagné. Associative alignment for few-shot image classification. In *Proceedings of the European Conference on Computer Vision (ECCV)*, 2020. 2, 5, 6
- [3] Arman Afrasiyabi, Jean-François Lalonde, and Christian Gagné. Mixture-based feature space learning for few-shot image classification. In *Proceedings of the IEEE/CVF International Conference on Computer Vision*, pages 9041–9051, 2021. 3, 6

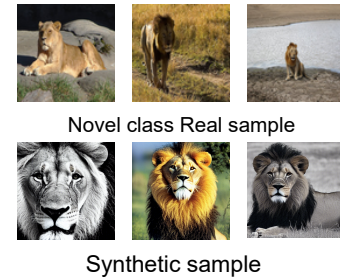
- [4] Arman Afrasiyabi, Hugo Larochelle, Jean-François Lalonde, and Christian Gagné. Matching feature sets for few-shot image classification. *arXiv preprint arXiv:2204.00949*, 2022. 3
- [5] Luca Bertinetto, Joao F. Henriques, Philip Torr, and Andrea Vedaldi. Meta-learning with differentiable closed-form solvers. In *International Conference on Learning Representations*, 2019. 5
- [6] Quentin Bouniot, Ievgen Redko, Romaric Audigier, Angélique Loesch, and Amaury Habrard. Improving few-shot learning through multi-task representation learning theory. In *European Conference on Computer Vision*, pages 435–452. Springer, 2022. 2
- [7] Tom Brown, Benjamin Mann, Nick Ryder, Melanie Subbiah, Jared D Kaplan, Prafulla Dhariwal, Arvind Neelakantan, Pranav Shyam, Girish Sastry, Amanda Askell, et al. Language models are few-shot learners. *Advances in neural information processing systems*, 33:1877–1901, 2020. 3
- [8] Kaidi Cao, Maria Brbic, and Jure Leskovec. Concept learners for few-shot learning. In *International Conference on Learning Representations*, 2021. 2
- [9] Wei-Yu Chen, Yen-Cheng Liu, Zsolt Kira, Yu-Chiang Frank Wang, and Jia-Bin Huang. A closer look at few-shot classification. *arXiv preprint arXiv:1904.04232*, 2019. 6
- [10] Philip Chikontwe, Soopil Kim, and Sang Hyun Park. Cad: Co-adapting discriminative features for improved few-shot classification. In *Proceedings of the IEEE/CVF Conference on Computer Vision and Pattern Recognition*, pages 14554–14563, 2022. 2
- [11] Suresh Dara, Swetha Dhamecherla, Surender Singh Jadav, CH Babu, and Mohamed Jawed Ahsan. Machine learning in drug discovery: a review. *Artificial Intelligence Review*, pages 1–53, 2021. 1
- [12] Rajshekhar Das, Yu-Xiong Wang, and José MF Moura. On the importance of distractors for few-shot classification. In *Proceedings of the IEEE/CVF International Conference on Computer Vision*, pages 9030–9040, 2021. 6
- [13] J. Deng, W. Dong, R. Socher, L. Li, Kai Li, and Li Fei-Fei. Imagenet: A large-scale hierarchical image database.



(a) Per-class accuracy without MMD (Avg. accuracy: 86.2%)



(b) Per-class accuracy improves with MMD (Avg. accuracy: 87.6%)



(c) Real and synthetic images shows domain gap. i.e., variation of chrominance.

Figure 6. Failure analysis of a randomly sampled episode: (a) and (b) shows the per-class accuracy without MMD loss and with MMD loss respectively. Sampled classes are - African hunting dog (label 0), Malamute (label 1), Lion (label 2), Vase (label 3), Crate (label 4) drawn from miniImageNet. (c) shows domain gap in terms of chrominance between the real and synthetic samples.

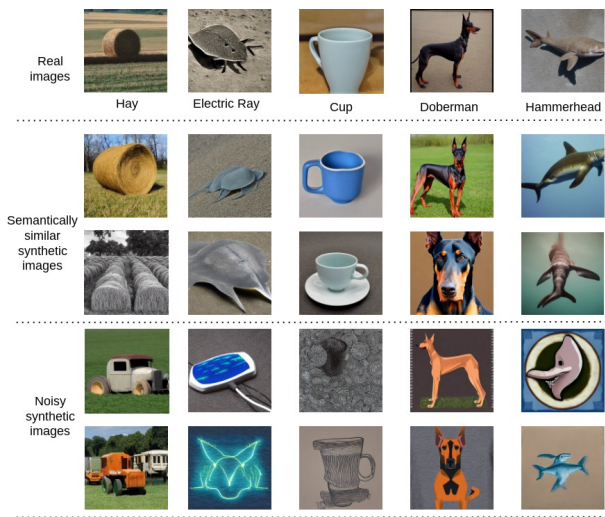


Figure 7. Real and generated images from tieredImageNet dataset. The first row shows the real images. In second and third row, we present semantically similar synthetic images. In the fourth and fifth row, we present some noisy images.

In 2009 *IEEE Conference on Computer Vision and Pattern Recognition*, 2009. 2

- [14] Nanyi Fei, Zhiwu Lu, Tao Xiang, and Songfang Huang. {MELR}: Meta-learning via modeling episode-level relationships for few-shot learning. In *International Conference on Learning Representations*, 2021. 6
- [15] Chelsea Finn, Pieter Abbeel, and Sergey Levine. Model-agnostic meta-learning for fast adaptation of deep networks. In *Proceedings of the 34th International Conference on Machine Learning*, pages 1126–1135, 2017. 2
- [16] Yizhao Gao, Nanyi Fei, Guangzhen Liu, Zhiwu Lu, Tao Xiang, and Songfang Huang. Contrastive prototype learning

with augmented embeddings for few-shot learning. *arXiv preprint arXiv:2101.09499*, 2021. 5

- [17] Ian Goodfellow, Jean Pouget-Abadie, Mehdi Mirza, Bing Xu, David Warde-Farley, Sherjil Ozair, Aaron Courville, and Yoshua Bengio. Generative adversarial networks. *Communications of the ACM*, 63(11):139–144, 2020. 4
- [18] Kaiming He, Xiangyu Zhang, Shaoqing Ren, and Jian Sun. Deep residual learning for image recognition. In *Proceedings of the IEEE Conference on Computer Vision and Pattern Recognition (CVPR)*, 2016. 2, 3
- [19] Jonathan Ho, Ajay Jain, and Pieter Abbeel. Denoising diffusion probabilistic models. *Advances in Neural Information Processing Systems*, 33:6840–6851, 2020. 3, 4
- [20] Shell Xu Hu, Da Li, Jan Stühmer, Minyoung Kim, and Timothy M Hospedales. Pushing the limits of simple pipelines for few-shot learning: External data and fine-tuning make a difference. In *Proceedings of the IEEE/CVF Conference on Computer Vision and Pattern Recognition*, pages 9068–9077, 2022. 2
- [21] Yiren Jian and Lorenzo Torresani. Label hallucination for few-shot classification. In *Proceedings of the AAAI Conference on Artificial Intelligence*, 2022. 2, 3, 5, 6
- [22] Ivan Kobyzev, Simon JD Prince, and Marcus A Brubaker. Normalizing flows: An introduction and review of current methods. *IEEE transactions on pattern analysis and machine intelligence*, 43(11):3964–3979, 2020. 4
- [23] Alex Krizhevsky, Ilya Sutskever, and Geoffrey E Hinton. Imagenet classification with deep convolutional neural networks. In *Advances in Neural Information Processing Systems*, 2012. 2
- [24] Prashant Kumar, Kushal Sinha, Nandkishor K Nere, Yujin Shin, Raimundo Ho, Laurie B Mlinar, and Ahmad Y Sheikh. A machine learning framework for computationally expensive transient models. *Scientific reports*, 10(1):1–11, 2020. 1

- [25] Kwonjoon Lee, Subhansu Maji, Avinash Ravichandran, and Stefano Soatto. Meta-learning with differentiable convex optimization. In *Proceedings of the IEEE/CVF Conference on Computer Vision and Pattern Recognition (CVPR)*, 2019. 5, 6
- [26] Bin Liu, Yue Cao, Yutong Lin, Qi Li, Zheng Zhang, Mingsheng Long, and Han Hu. Negative margin matters: Understanding margin in few-shot classification. In Andrea Vedaldi, Horst Bischof, Thomas Brox, and Jan-Michael Frahm, editors, *Computer Vision – ECCV 2020*, 2020. 6
- [27] Yang Liu, Weifeng Zhang, Chao Xiang, Tu Zheng, Deng Cai, and Xiaofei He. Learning to affiliate: Mutual centralized learning for few-shot classification. In *Proceedings of the IEEE/CVF Conference on Computer Vision and Pattern Recognition*, pages 14411–14420, 2022. 2
- [28] Mingsheng Long, Yue Cao, Jianmin Wang, and Michael Jordan. Learning transferable features with deep adaptation networks. In *International conference on machine learning*, pages 97–105. PMLR, 2015. 2, 4
- [29] Jiawei Ma, Hanchen Xie, Guangxing Han, Shih-Fu Chang, Aram Galstyan, and Wael Abd-Almageed. Partner-assisted learning for few-shot image classification. In *Proceedings of the IEEE/CVF International Conference on Computer Vision*, pages 10573–10582, 2021. 2, 5
- [30] Rongkai Ma, Pengfei Fang, Gil Avraham, Yan Zuo, Tianyu Zhu, Tom Drummond, and Mehrtash Harandi. Learning instance and task-aware dynamic kernels for few-shot learning. In *European Conference on Computer Vision*, pages 257–274. Springer, 2022. 2
- [31] Puneet Mangla, Nupur Kumari, Abhishek Sinha, Mayank Singh, Balaji Krishnamurthy, and Vineeth N Balasubramanian. Charting the right manifold: Manifold mixup for few-shot learning. In *Proceedings of the IEEE/CVF Winter Conference on Applications of Computer Vision*, pages 2218–2227, 2020. 6
- [32] Alex Nichol, Prafulla Dhariwal, Aditya Ramesh, Pranav Shyam, Pamela Mishkin, Bob McGrew, Ilya Sutskever, and Mark Chen. Glide: Towards photorealistic image generation and editing with text-guided diffusion models. *arXiv preprint arXiv:2112.10741*, 2021. 3, 4
- [33] Boris N. Oreshkin, Pau Rodríguez López, and Alexandre Lacoste. Tadam: Task dependent adaptive metric for improved few-shot learning. In *NeurIPS*, 2018. 2, 5, 6
- [34] Frederik Pahde, Mihai Puscas, Tassilo Klein, and Moin Nabi. Multimodal prototypical networks for few-shot learning. In *Proceedings of the IEEE/CVF Winter Conference on Applications of Computer Vision*, pages 2644–2653, 2021. 3, 4
- [35] Alec Radford, Jong Wook Kim, Chris Hallacy, Aditya Ramesh, Gabriel Goh, Sandhini Agarwal, Girish Sastry, Amanda Askell, Pamela Mishkin, Jack Clark, et al. Learning transferable visual models from natural language supervision. In *International Conference on Machine Learning*, pages 8748–8763. PMLR, 2021. 3, 4
- [36] Jathushan Rajasegaran, Salman Khan, Munawar Hayat, Fahad Shahbaz Khan, and Mubarak Shah. Self-supervised knowledge distillation for few-shot learning. *arXiv preprint arXiv:2006.09785*, 2020. 2, 5, 6
- [37] Aditya Ramesh, Prafulla Dhariwal, Alex Nichol, Casey Chu, and Mark Chen. Hierarchical text-conditional image generation with clip latents. *arXiv preprint arXiv:2204.06125*, 2022. 2, 3, 4
- [38] Avinash Ravichandran, Rahul Bhotika, and Stefano Soatto. Few-shot learning with embedded class models and shot-free meta training. In *Proceedings of the IEEE/CVF International Conference on Computer Vision (ICCV)*, 2019. 2, 5, 6
- [39] Mengye Ren, Sachin Ravi, Eleni Triantafillou, Jake Snell, Kevin Swersky, Josh B. Tenenbaum, Hugo Larochelle, and Richard S. Zemel. Meta-learning for semi-supervised few-shot classification. In *International Conference on Learning Representations*, 2018. 5
- [40] Mamshad Nayeem Rizve, Salman Khan, Fahad Shahbaz Khan, and Mubarak Shah. Exploring complementary strengths of invariant and equivariant representations for few-shot learning. *arXiv preprint arXiv:2103.01315*, 2021. 2, 3, 5, 6
- [41] Robin Rombach, Andreas Blattmann, Dominik Lorenz, Patrick Esser, and Björn Ommer. High-resolution image synthesis with latent diffusion models. In *Proceedings of the IEEE/CVF Conference on Computer Vision and Pattern Recognition*, pages 10684–10695, 2022. 1, 2, 3, 4
- [42] Olaf Ronneberger, Philipp Fischer, and Thomas Brox. U-net: Convolutional networks for biomedical image segmentation. In *International Conference on Medical image computing and computer-assisted intervention*, pages 234–241. Springer, 2015. 4
- [43] Aniket Roy, Anshul Shah, Ketul Shah, Prithviraj Dhar, Anoop Cherian, and Rama Chellappa. FeLMi : Few shot learning with hard mixup. In Alice H. Oh, Alekh Agarwal, Danielle Belgrave, and Kyunghyun Cho, editors, *Advances in Neural Information Processing Systems*, 2022. 2, 3, 5, 6
- [44] Andrei A. Rusu, Dushyant Rao, Jakub Sygnowski, Oriol Vinyals, Razvan Pascanu, Simon Osindero, and Raia Hadsell. Meta-learning with latent embedding optimization. In *International Conference on Learning Representations*, 2019. 2
- [45] Zhiqiang Shen, Zechun Liu, Jie Qin, Marios Savvides, and Kwang-Ting Cheng. Partial is better than all: Revisiting fine-tuning strategy for few-shot learning. *CoRR*, abs/2102.03983, 2021. 6
- [46] Christian Simon, Piotr Koniusz, Richard Nock, and Mehrtash Harandi. Adaptive subspaces for few-shot learning. In *Proceedings of the IEEE/CVF Conference on Computer Vision and Pattern Recognition (CVPR)*, 2020. 5, 6
- [47] Jake Snell, Kevin Swersky, and Richard Zemel. Prototypical networks for few-shot learning. In *Advances in Neural Information Processing Systems*, 2017. 2, 5, 6
- [48] Qianru Sun, Yaoyao Liu, Tat-Seng Chua, and Bernt Schiele. Meta-transfer learning for few-shot learning. In *Proceedings of the IEEE/CVF Conference on Computer Vision and Pattern Recognition (CVPR)*, 2019. 5, 6
- [49] Flood Sung, Yongxin Yang, Li Zhang, Tao Xiang, Philip H.S. Torr, and Timothy M. Hospedales. Learning to compare: Relation network for few-shot learning. In *Proceedings of the IEEE Conference on Computer Vision and Pattern Recognition (CVPR)*, 2018. 2

- [50] Yonglong Tian, Yue Wang, Dilip Krishnan, Joshua B. Tenenbaum, and Phillip Isola. Rethinking few-shot image classification: A good embedding is all you need? In Andrea Vedaldi, Horst Bischof, Thomas Brox, and Jan-Michael Frahm, editors, *Computer Vision – ECCV 2020*, 2020. 1, 2, 5, 6
- [51] Oriol Vinyals, Charles Blundell, Timothy Lillicrap, koray kavukcuoglu, and Daan Wierstra. Matching networks for one shot learning. In *Advances in Neural Information Processing Systems*, 2016. 2, 5
- [52] Shuo Wang, Xinyu Zhang, Yanbin Hao, Chengbing Wang, and Xiangnan He. Multi-directional knowledge transfer for few-shot learning. In *Proceedings of the 30th ACM International Conference on Multimedia*, pages 3993–4002, 2022. 3
- [53] Jingyi Xu and Hieu Le. Generating representative samples for few-shot classification. In *Proceedings of the IEEE/CVF Conference on Computer Vision and Pattern Recognition*, pages 9003–9013, 2022. 3, 4, 5, 6
- [54] Fengyuan Yang, Ruiping Wang, and Xilin Chen. Sega: semantic guided attention on visual prototype for few-shot learning. In *Proceedings of the IEEE/CVF Winter Conference on Applications of Computer Vision*, pages 1056–1066, 2022. 3, 5, 6
- [55] Zhanyuan Yang, Jinghua Wang, and Yingying Zhu. Few-shot classification with contrastive learning. In *European Conference on Computer Vision*, pages 293–309. Springer, 2022. 2, 4
- [56] Han-Jia Ye, Hexiang Hu, De-Chuan Zhan, and Fei Sha. Few-shot learning via embedding adaptation with set-to-set functions. In *Proceedings of the IEEE/CVF Conference on Computer Vision and Pattern Recognition (CVPR)*, 2020. 2, 6
- [57] Sung Whan Yoon, Jun Seo, and Jaekyun Moon. TapNet: Neural network augmented with task-adaptive projection for few-shot learning. In *Proceedings of the 36th International Conference on Machine Learning*, Proceedings of Machine Learning Research, pages 7115–7123. PMLR, 09–15 Jun 2019. 6
- [58] Baoquan Zhang, Xutao Li, Yunming Ye, Zhichao Huang, and Lisai Zhang. Prototype completion with primitive knowledge for few-shot learning. In *Proceedings of the IEEE/CVF Conference on Computer Vision and Pattern Recognition*, pages 3754–3762, 2021. 3
- [59] Chi Zhang, Yujun Cai, Guosheng Lin, and Chunhua Shen. Deepemd: Few-shot image classification with differentiable earth mover’s distance and structured classifiers. In *IEEE/CVF Conference on Computer Vision and Pattern Recognition (CVPR)*, 2020. 2, 5, 6
- [60] Manli Zhang, Jianhong Zhang, Zhiwu Lu, Tao Xiang, Mingyu Ding, and Songfang Huang. {IEPT}: Instance-level and episode-level pretext tasks for few-shot learning. In *International Conference on Learning Representations*, 2021. 6
- [61] Renrui Zhang, Wei Zhang, Rongyao Fang, Peng Gao, Kunchang Li, Jifeng Dai, Yu Qiao, and Hongsheng Li. Tip-adapter: Training-free adaption of clip for few-shot classification. In *European Conference on Computer Vision*, pages 493–510. Springer, 2022. 2
- [62] Kaiyang Zhou, Jingkang Yang, Chen Change Loy, and Ziwei Liu. Learning to prompt for vision-language models. *International Journal of Computer Vision*, 130(9):2337–2348, 2022. 4
- [63] Hao Zhu and Piotr Koniusz. Ease: Unsupervised discriminant subspace learning for transductive few-shot learning. In *Proceedings of the IEEE/CVF Conference on Computer Vision and Pattern Recognition*, pages 9078–9088, 2022. 2